

# Synthesis of Framework Lithium Zirconium Molybdate Phosphates and Their Catalytic Properties in Ethanol Conversion Reactions

A. B. Il'in<sup>a, b</sup>, M. M. Ermilova<sup>a</sup>, N. V. Orekhova<sup>a</sup>, and A. B. Yaroslavtsev<sup>a, b</sup>

<sup>a</sup> Topchiev Institute of Petrochemical Synthesis, Russian Academy of Sciences,  
Leninskii pr. 29, Moscow, 119991 Russia

<sup>b</sup> Kurnakov Institute of General and Inorganic Chemistry, Russian Academy of Sciences,  
Leninskii pr. 31, Moscow, 119991 Russia

e-mail: yaroslav@igic.ras.ru

Received January 20, 2015

**Abstract**—We have synthesized NASICON-type mixed phosphates with the general formula  $\text{Li}_{1-x}\text{Zr}_2\text{P}_{3-x}\text{Mo}_x\text{O}_{12}$ , having different degrees of molybdenum substitution ( $x = 0, 0.1, 0.5, 1.0$ ) and ranging in particle size from 50 to 300 nm. Their structure and morphology have been investigated using X-ray diffraction, scanning electron microscopy, and X-ray microanalysis. Analysis of the catalytic properties of the synthesized compounds in ethanol conversion reactions demonstrates that all of them exhibit catalytic activity for ethanol dehydration and dehydrogenation reactions and that the relationship between them depends on molybdenum content.

**DOI:** 10.1134/S0020168515070055

## INTRODUCTION

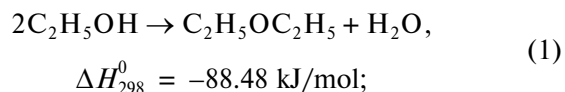
In the last decade, one priority issue has been the development of green chemistry, connected with a search for environmentally clean ways of producing practically important substances and materials. A great deal of attention has been paid to the use of renewable sources of energy and raw materials [1]. In connection with this, biomass, whose intermediate processing products are bioalcohols, is often regarded as a promising energy source. Bioalcohols can, however, be regarded not only as promising fuels but also as raw materials for the chemical industry. For this reason, there is currently great practical interest in a search for and development of catalysts capable of converting alcohols to products of industrial importance, such as hydrogen, hydrocarbons, ethers, aldehydes, and ketones [2].

NASICON (acronym for Na Super Ionic CONductor) materials received their name owing to the discovery by Hong that zirconium sodium silicate phosphates have high ionic conductivity [3–5]. This class of compounds can be described by the general formula  $\text{A}_x\text{B}_2(\text{ZO}_4)_3$ , where A is usually an alkali or alkaline-earth metal, B is a polyvalent element (Zr, Ti, In, or others), and Z is phosphorus or silicon. Their structure is made up of  $\text{BO}_6$  octahedra and  $\text{ZO}_4$  tetrahedra, which are linked so that there are spacious voids forming a three-dimensional network of channels. Some of these voids are occupied by the A cations [6]. Owing to this, these materials possess a number of

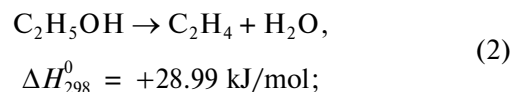
valuable properties, such as high ionic conductivity and variability of their framework structure, which enable iso- or heterovalent substitutions on both the cation and anion sites, without significant structural changes [7, 8].

Such substitutions may also be useful in catalysis because they allow one to vary the concentration and strength of Lewis and Bronsted acid centers. The large fraction of covalent bonding in framework compounds contributes to their high thermal stability, stability to high temperatures, and chemical stability, for example, to water and sulfur oxides, which is of particular importance for catalysts. It has been shown in a number of studies [[9–16] that NASICON-type compounds are active in acid and redox catalysis processes. Owing to this, conversion of ethanol may follow a few alternative paths:

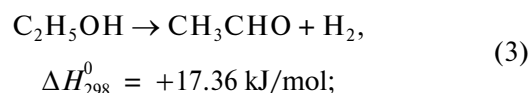
dehydration to diethyl ether (DEE),



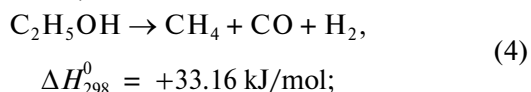
dehydration to ethylene,



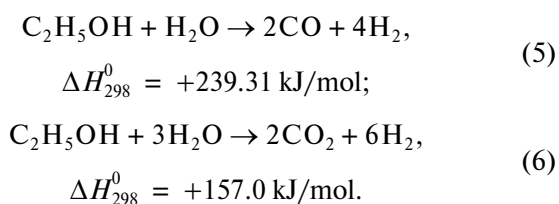
dehydrogenation to acetaldehyde,



methanation,



steam reforming,



Also possible are the dehydrogenation of the reaction products and the catalytic cross-linking of the forming unsaturated hydrocarbons.

In this study, major attention is paid to the effect of heterovalent doping on the catalytic activity of  $\text{LiZr}_2(\text{PO}_4)_3$ -based NASICON-type materials. According to Pylina and Mikhalenko [17], the surface of such compounds is formed largely by phosphate anions, and it is reasonable to expect that their catalytic activity in heterogeneous catalysis processes is most sensitive to partial substitutions on the phosphorus site. As a dopant, we chose molybdenum, which has a variable oxidation state and readily forms tetrahedral anions [18]. The main purpose of this work was to assess the catalytic activity of framework materials with the compositions  $\text{Li}_{1-x}\text{Zr}_2\text{P}_{3-x}\text{Mo}_x\text{O}_{12}$  ( $x = 0, 0.1, 0.5, 1.0$ ) for the conversion of alcohols, as exemplified by ethanol. Understanding such a process allows one to assess the effects of the qualitative and quantitative compositions of the framework phosphates on the relationship between acid–base and redox centers on their surface.

## EXPERIMENTAL

The  $\text{Li}_{1-x}\text{Zr}_2\text{P}_{3-x}\text{Mo}_x\text{O}_{12}$  ( $x = 0, 0.1, 0.5, 1.0$ ) framework phosphates were prepared by the Pechini process [19, 20]. In a mixture of ethylene glycol (2 mL) and deionized water (10 mL) in an alumina crucible we sequentially dissolved  $\text{ZrOCl}_2 \cdot 8\text{H}_2\text{O}$ , citric acid,  $\text{Li}_2\text{CO}_3$ , and a stoichiometric mixture of  $\text{NH}_4\text{H}_2\text{PO}_4$  and  $(\text{NH}_4)_6\text{Mo}_7\text{O}_{24}$  corresponding to the phosphorus : molybdenum ratio in the compound to be synthesized. After that, the pH of the solution was rapidly brought to 5.5 by adding concentrated aqueous ammonia in order to prevent zirconium phosphate precipitation. The resultant solution was held in a drying oven at 95°C for 24 h, at 150°C for another 24 h, and then at 350°C for 4 h. After careful grinding, the material was annealed at 750°C for 10 h. The first steps led to a stepwise removal of water and other gaseous products. The final anneal determined the structure of the material.

The phase composition of the materials was determined by X-ray diffraction on a Rigaku D/MAX 2200 X-ray diffractometer ( $\text{CuK}\alpha_1$  radiation). Diffraction

patterns were analyzed using the Rigaku Application Data Processing software package.

The particle (crystallite) size was assessed from the broadening of X-ray diffraction peaks using the Scherrer formula:

$$D = \frac{k\lambda}{(B - b)\cos\theta}, \quad (7)$$

where  $k = 0.89$  is the Scherrer constant,  $\lambda = 1.5406 \text{ \AA}$  is the X-ray wavelength used,  $B$  is the half width at half maximum of the peak ( $2\theta$ ),  $b$  is the instrumental broadening ( $2\theta$ ), and  $\theta$  is the angular peak position. As a standard for evaluating the instrumental broadening, we used lanthanum hexaboride,  $\text{LaB}_6$ , powder (Standard Reference Material 660a).

The specific surface area of the samples was determined by BET measurements with a Micromeritics ASAP 2020 analyzer. The samples were degassed at a temperature of 350°C for 1 h. Analyses were carried out at relative pressures ( $p/p_0$ ) from 0.01 to 0.99.

The samples were examined by scanning electron microscopy (SEM) on a Carl Zeiss NVision 40 equipped with an elemental analysis accessory. The accelerating voltage was 1 kV.

Catalytic properties were studied in a flow-type quartz reactor under saturated ethanol vapor. The reaction products were analyzed on a Kristallyuks 4000M chromatograph equipped with a thermal conductivity detector and HayeSep T 60/80 mesh (2 m, 150°C, 30 mL/min, He), SKT-6 (2 m, 150°C, 30 mL/min, He), and Molecular sieve 5 A (2 m, 25°C, 30 mL/min, Ar) columns. In our experiments, a weighed amount (0.3 g) of a catalyst was mixed with ground quartz ( $d = 315\text{--}400 \text{ }\mu\text{m}$ ) and placed in a reactor 6 mm in inner diameter so that the catalyst layer was 17 cm in thickness. To ensure an appropriate ethanol vapor concentration, the carrier gas was passed at a volumetric flow rate of 20 mL/min through a bubbler containing ethanol and thermostated at 11°C.

The catalytic activity of the samples was assessed as the amount of the corresponding reaction product (in millimoles) forming per gram of the catalyst per hour. The selectivity of the samples was evaluated by the formula

$$S = \frac{\varphi_{\text{prod}} n_{\text{prod}}}{\varphi_{\text{alcohol}} n_{\text{alcohol}}}, \quad (8)$$

where  $\varphi_{\text{prod/alcohol}}$  is the volume fraction of the reaction product and reacted alcohol, respectively, and  $n_{\text{prod/alcohol}}$  is the number of carbon atoms per molecule of the reaction product and alcohol, respectively.

## RESULTS AND DISCUSSION

According to electron probe microanalysis data (table), the elemental composition of the synthesized materials corresponded to the intended stoichiometry. According to X-ray diffraction data, all of the samples

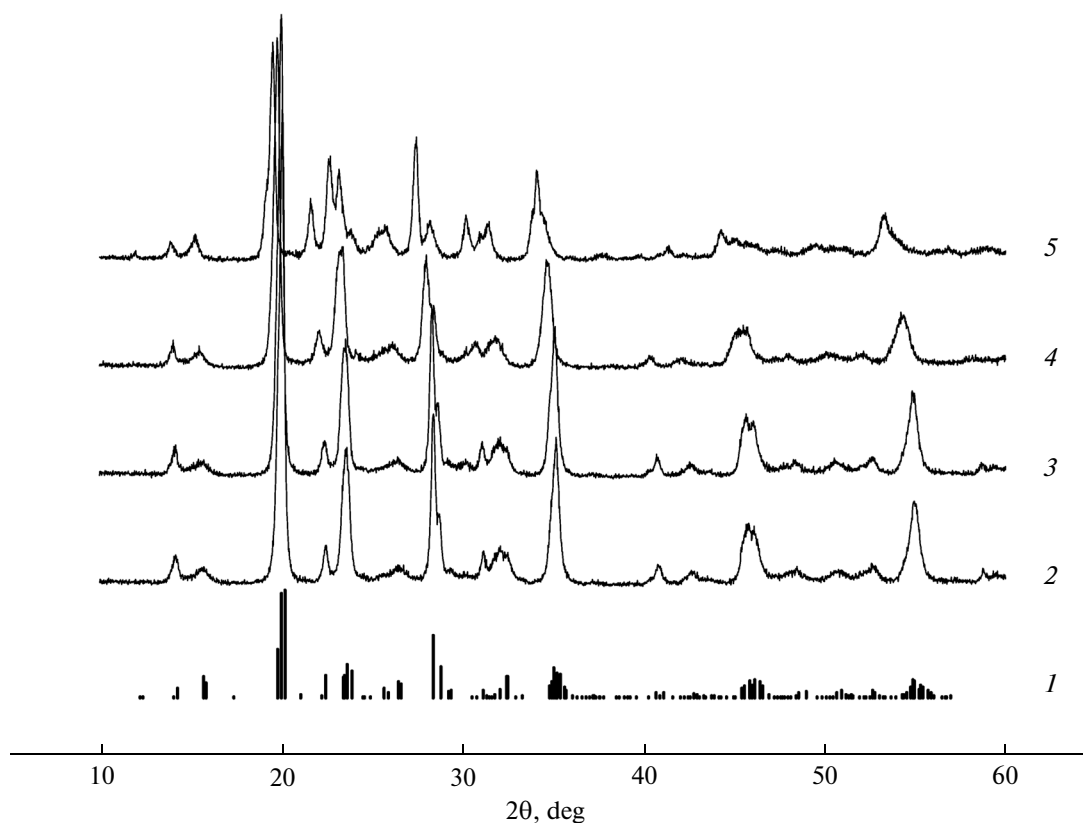


**Fig. 1.** X-ray diffraction patterns of the synthesized compounds: (1) schematic X-ray diffraction pattern of monoclinic  $\text{LiZr}_2(\text{PO}_4)_3$  (card no. 70-5819), (2)  $\text{LiZr}_2(\text{PO}_4)_3$ , (3)  $\text{Li}_{0.9}\text{Zr}_2\text{P}_{2.9}\text{Mo}_{0.1}\text{O}_{12}$ , (4)  $\text{Li}_{0.5}\text{Zr}_2\text{P}_{2.5}\text{Mo}_{0.5}\text{O}_{12}$ , (5)  $\text{Zr}_2\text{P}_2\text{MoO}_{12}$ .

were single-phase and had a monoclinic NASICON-related structure (Fig. 1). Calculations showed that the samples ranged in crystallite size from 20 to 50 nm (table). According to SEM data, the samples consisted of particles 50 to 300 nm in size (Fig. 2).

The materials had rather small specific surface areas, from 6 to 20  $\text{m}^2/\text{g}$  (table). The average particle sizes estimated from these data are also presented in the table, together with the estimated crystallite sizes. Comparison of these data leads us to conclude that the larger particles observed in SEM micrographs are agglomerates of individual crystallites. The same is evidenced by estimates from the specific surface area data.

Our experiments showed that all of the synthesized samples had considerable catalytic activity for ethanol dehydration and dehydrogenation reactions (Fig. 3a). The negligible conversion of ethanol in blank experiments with the use of silicon oxide indicated that it was the phosphates under investigation that exhibited the catalytic activity. The major reaction products were C2 hydrocarbons (ethane and ethylene), C4 hydrocarbons, acetaldehyde, diethyl ether, and hydrogen. We also observed the formation of trace amounts of C3 hydrocarbons,  $\text{CO}_2$ , and CO.

The molybdenum-free catalyst  $\text{LiZr}_2(\text{PO}_4)_3$  showed the highest selectivity for ethanol dehydration to diethyl ether and C2 hydrocarbons (Figs. 3b, 3e) because of the high acidity and the absence of well-

Specific surface area of the synthesized compounds and their characteristic particle size evaluated by different techniques

Composition	$S$ , $\text{m}^2/\text{g}$	$D_{\text{cr}}$ , nm	$d_{\text{av}}$ , nm
$\text{LiZr}_2(\text{PO}_4)_3$	$16 \pm 1$	$49 \pm 2$	115
$\text{Li}_{0.9}\text{Zr}_2\text{P}_{2.9}\text{Mo}_{0.1}\text{O}_{12}$	$20 \pm 1$	$40 \pm 2$	94
$\text{Li}_{0.5}\text{Zr}_2\text{P}_{2.5}\text{Mo}_{0.5}\text{O}_{12}$	$6.8 \pm 0.7$	$23 \pm 1$	261
$\text{Zr}_2\text{P}_2\text{MoO}_{12}$	$5.8 \pm 0.6$	$48 \pm 2$	288

$d_{\text{av}}$  is the average particle size evaluated from the specific surface area.

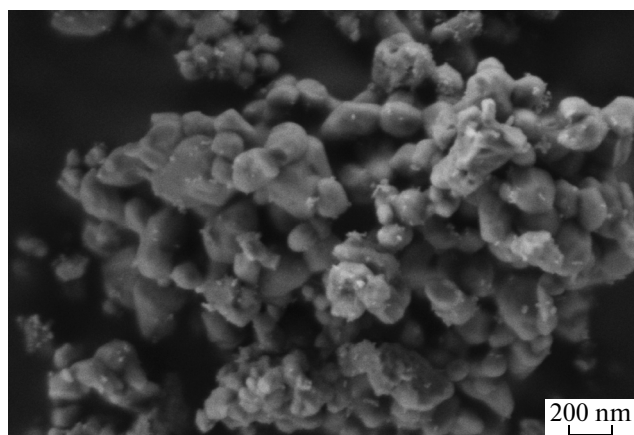


**Fig. 2.** Micrograph of a sample with the composition  $\text{Zr}_2\text{P}_2\text{MoO}_{12}$ .

defined redox centers. The ethanol dehydrogenation product, acetaldehyde, forms on  $\text{LiZr}_2(\text{PO}_4)_3$  in trace amounts and only at temperatures above  $300^\circ\text{C}$ .

At the same time, as a result of the incorporation of molybdenum into the structure of the phosphate, degrees of ethanol conversion equivalent to those for the undoped material were observed at temperatures on average  $60^\circ\text{C}$  lower in comparison with undoped  $\text{LiZr}_2(\text{PO}_4)_3$  (Fig. 3a). This was accompanied by an increase in the rate of redox processes, including dehydrogenation and catalytic cross-linking. The addition of a small amount of molybdenum enables lower temperature formation of C2 and C4 hydrocarbons in amounts that can only be reached on the  $\text{LiZr}_2(\text{PO}_4)_3$  sample at temperatures in the range  $300\text{--}350^\circ\text{C}$  (Figs. 3b, 3c). Doping has the strongest effect on the acetaldehyde, diethyl ether, and hydrogen yields (Fig. 3). Note that the effects for the acetaldehyde and diethyl ether yields are almost identical for all of the doped samples. The acetaldehyde yield increases by approximately a factor of 8, whereas the diethyl ether yield, in contrast, drops by almost a factor of 3. The formation of hydrogen passes through a maximum for the sample with the composition  $\text{Li}_{0.9}\text{Zr}_2\text{P}_{2.9}\text{Mo}_{0.1}\text{O}_{12}$ , which ensures an increase in yield by more than a factor of 5. At the same time, this parameter decreases to 3 for  $\text{Li}_{0.5}\text{Zr}_2\text{P}_{2.5}\text{Mo}_{0.5}\text{O}_{12}$  and  $\text{Zr}_2\text{P}_2\text{MoO}_{12}$ .

One possible cause of the drop in the diethyl ether yield at even low molybdenum doping levels is that the process in question requires that there be two neighboring phosphorus groups necessary for the sorption of two alcohol molecules. This condition can be substantially violated in the presence of even low molybdenum concentrations because of the predominant molybdenum localization on the sample surface.

The formation of C4 hydrocarbons also passes through a maximum, even though the maximum values do not reach those for the undoped material

(Fig. 3c). The similarity in properties between  $\text{Li}_{0.5}\text{Zr}_2\text{P}_{2.5}\text{Mo}_{0.5}\text{O}_{12}$  and  $\text{Zr}_2\text{P}_2\text{MoO}_{12}$  can be accounted for by the fact that these materials are close in specific surface area: 6.8 and  $5.8\text{ m}^2/\text{g}$ , respectively. The specific surface area of  $\text{Li}_{0.9}\text{Zr}_2\text{P}_{2.9}\text{Mo}_{0.1}\text{O}_{12}$  is three times larger and almost identical to that of  $\text{LiZr}_2(\text{PO}_4)_3$  (table).

Comparison of the specific surface area data and catalysis results leads us to conclude that the amount and activity of centers responsible for the formation of acetaldehyde and diethyl ether in the doped samples are essentially independent of molybdenum content, whereas, in the case of the other reaction products, these parameters of the centers differ, which has a particularly marked effect on the formation of C4 hydrocarbons and hydrogen.

It can be seen from Fig. 4 that the incorporation of molybdenum has a significant effect on the selectivity of the catalyst and the composition of the reaction products. Whereas the undoped material has the highest low-temperature selectivity for diethyl ether, the major reaction product in the case of the molybdenum-doped samples is acetaldehyde. At high temperatures, all of the samples are selective largely for the C2 and C4 hydrocarbons. Note that the temperature dependences of selectivity are similar in shape for all of the doped samples. The most drastic distinction is observed only for the C4 hydrocarbons: the selectivity of the  $\text{Li}_{0.9}\text{Zr}_2\text{P}_{2.9}\text{Mo}_{0.1}\text{O}_{12}$  sample for these hydrocarbons reaches 59%, whereas that of  $\text{Li}_{0.5}\text{Zr}_2\text{P}_{2.5}\text{Mo}_{0.5}\text{O}_{12}$  and  $\text{Zr}_2\text{P}_2\text{MoO}_{12}$  is slightly below 50%.

The nearly identical shape of the temperature dependences of selectivity for all of the doped samples, containing lithium and free of it ( $\text{Li}_{0.9}\text{Zr}_2\text{P}_{2.9}\text{Mo}_{0.1}\text{O}_{12}$ ,  $\text{Li}_{0.5}\text{Zr}_2\text{P}_{2.5}\text{Mo}_{0.5}\text{O}_{12}$ , and  $\text{Zr}_2\text{P}_2\text{MoO}_{12}$ ), suggests that they are close in the ratio between the amounts of acid and redox centers on their surface, which can be interpreted as indirect evidence for predominant molybdenum localization on the surface of the materials. This leads to relaxation processes and a reduction in the excess energy necessary for heterovalent substitution [21].

The temperature variation of the selectivity of the synthesized samples for hydrogen, which is one of the most attractive ethanol conversion products, is difficult to relate to any particular hydrogen release or absorption process. For this reason, these data are presented as the temperature dependence of the ratio between the amounts of released hydrogen and reacted ethanol (Fig. 5).

For all of the doped samples, this ratio has a minimum: at low degrees of conversion, all of the released hydrogen results from ethanol dehydrogenation to acetaldehyde, so the initial ratio should be close to unity. At the same time, the hydrogen/ethanol ratio does not exceed 0.6 even at the lowest process temperatures, and decreases further at higher temperatures, dropping to a minimum at temperatures near  $320^\circ\text{C}$ .

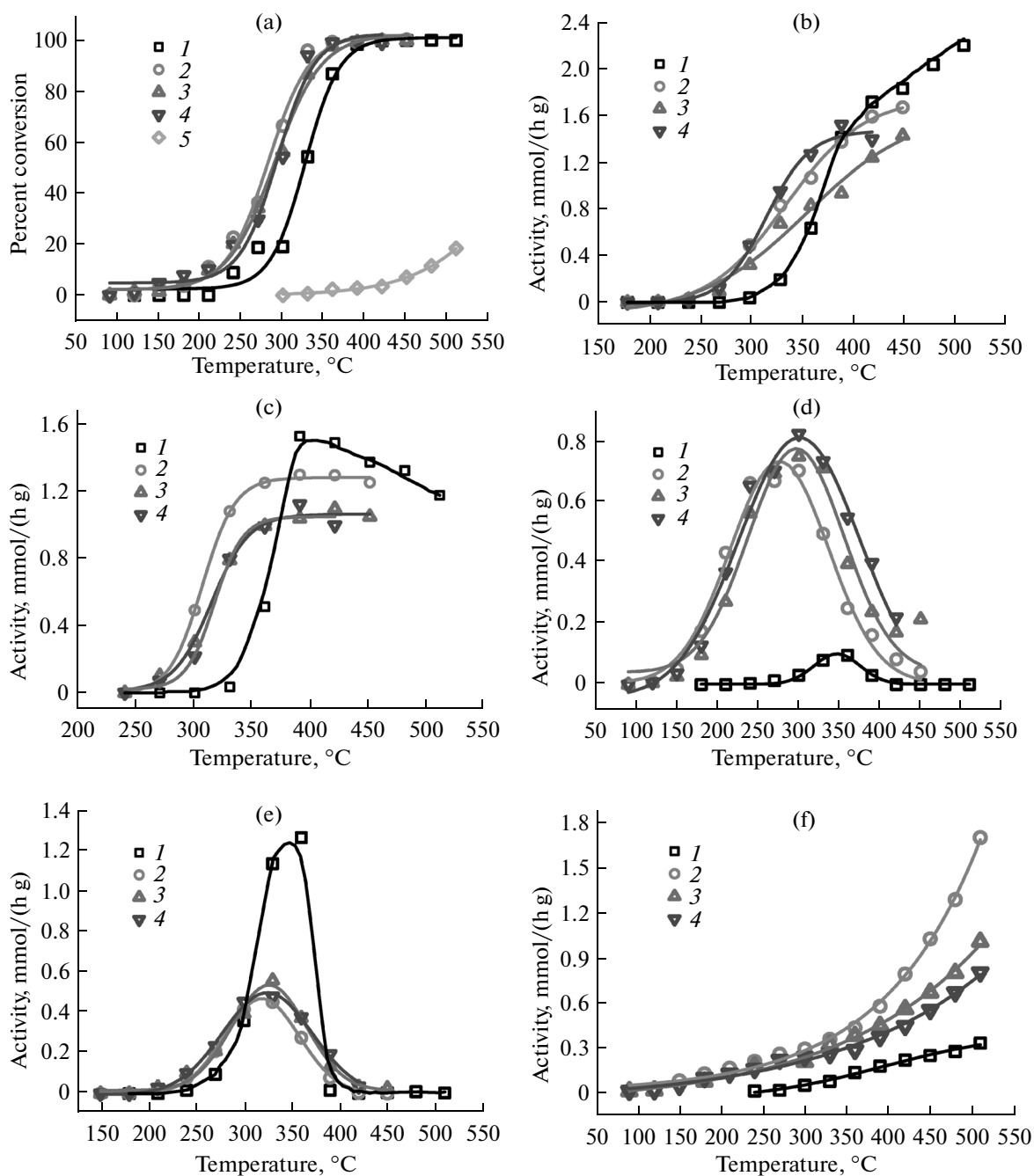


**Fig. 3.** Ethanol conversion as a function of temperature (a) and catalytic activity of molybdenum-doped samples for the formation of C<sub>2</sub> hydrocarbons (b), C<sub>4</sub> hydrocarbons (c), acetaldehyde (d), diethyl ether (e), and hydrogen (f): (1) LiZr<sub>2</sub>(PO<sub>4</sub>)<sub>3</sub>, (2) Li<sub>0.9</sub>Zr<sub>2</sub>P<sub>2.9</sub>Mo<sub>0.1</sub>O<sub>12</sub>, (3) Li<sub>0.5</sub>Zr<sub>2</sub>P<sub>2.5</sub>Mo<sub>0.5</sub>O<sub>12</sub>, (4) Zr<sub>2</sub>P<sub>2</sub>MoO<sub>12</sub>, (5) SiO<sub>2</sub> (blank experiment).

It seems likely that some of the hydrogen resulting from the dehydrogenation does not enter the gas phase but reduces the molybdenum. A similar effect was observed previously by Sukhanov et al. [22] for methanol conversion reactions on sodium zirconium molybdate phosphates in an argon atmosphere [22]. At high temperatures, the ratio of hydrogen to reacted ethanol increases considerably. In this case, reaction

by-products (hydrocarbons) act as hydrogen sources. The most active hydrogen release was observed for the sample with the composition Li<sub>0.9</sub>Zr<sub>2</sub>P<sub>2.9</sub>Mo<sub>0.1</sub>O<sub>12</sub> (Fig. 5). On the undoped sample, which offered far higher selectivity for the dehydration process, hydrogen was released starting at much higher temperatures, and the corresponding curve had no minimum (Fig. 5, curve 1).

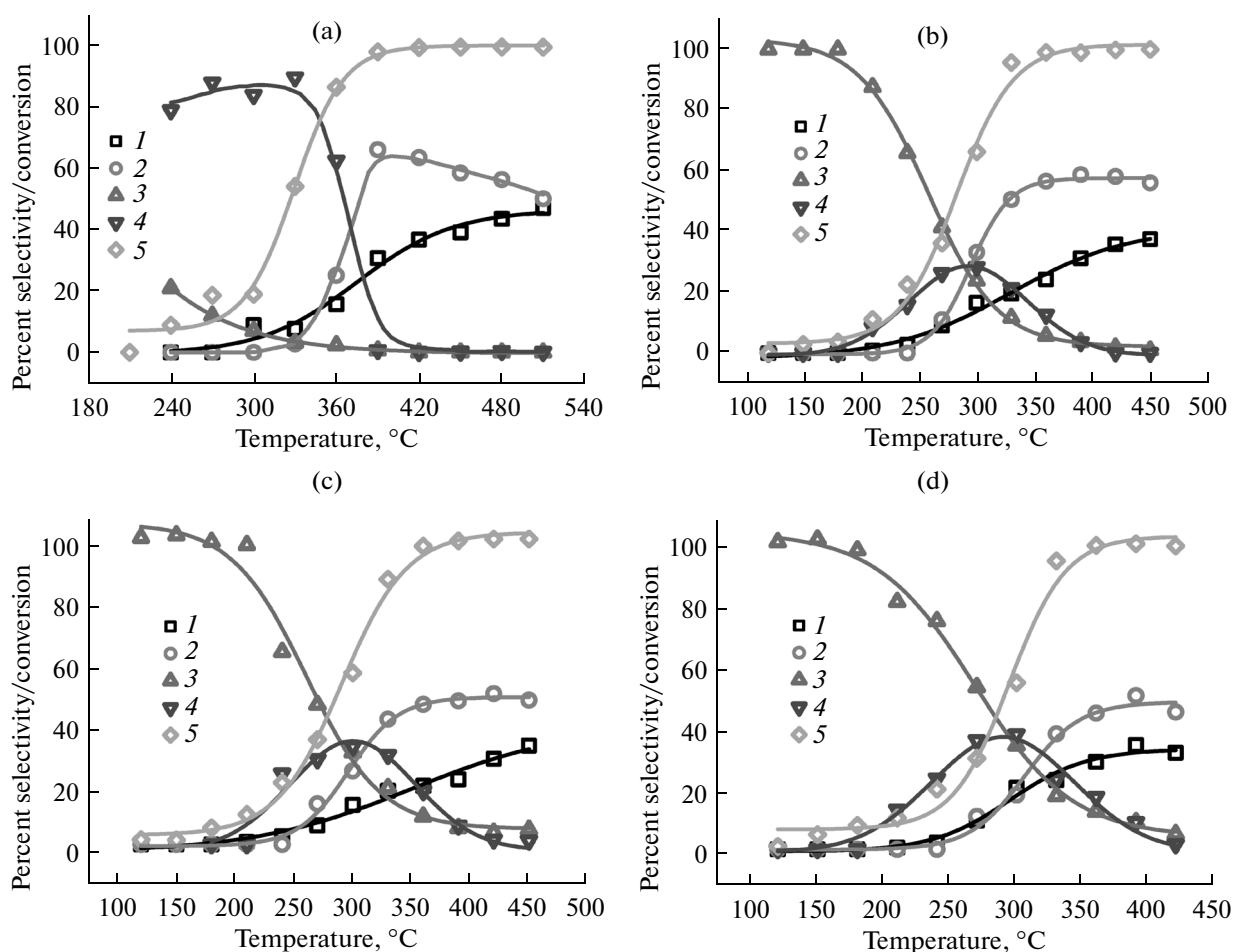


**Fig. 4.** Selectivity in the formation of (1) C2 hydrocarbons, (2) C4 hydrocarbons, (3) acetaldehyde, and (4) diethyl ether and (5) ethanol conversion as functions of temperature for samples with the compositions (a)  $\text{LiZr}_2(\text{PO}_4)_3$ , (b)  $\text{Li}_{0.9}\text{Zr}_2\text{P}_{2.9}\text{Mo}_{0.1}\text{O}_{12}$ , (c)  $\text{Li}_{0.5}\text{Zr}_2\text{P}_{2.5}\text{Mo}_{0.5}\text{O}_{12}$ , and (d)  $\text{Zr}_2\text{P}_2\text{MoO}_{12}$ .

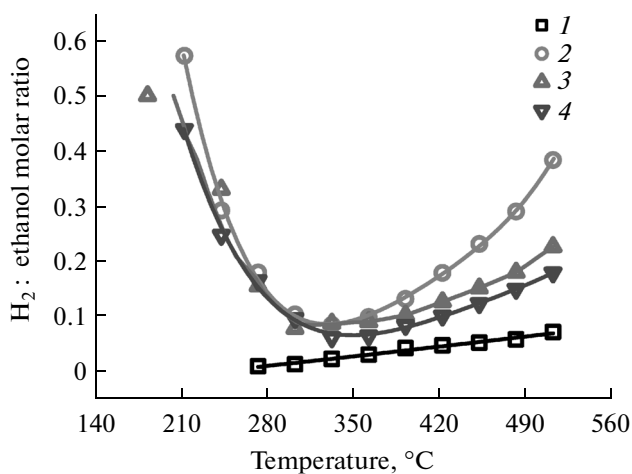


**Fig. 5.** Temperature dependences of the molar ratio of the hydrogen obtained in the reaction to the reacted ethanol: (1)  $\text{LiZr}_2(\text{PO}_4)_3$ , (2)  $\text{Li}_{0.9}\text{Zr}_2\text{P}_{2.9}\text{Mo}_{0.1}\text{O}_{12}$ , (3)  $\text{Li}_{0.5}\text{Zr}_2\text{P}_{2.5}\text{Mo}_{0.5}\text{O}_{12}$ , (4)  $\text{Zr}_2\text{P}_2\text{MoO}_{12}$ .

## CONCLUSIONS

We have synthesized single-phase nanoparticulate molybdenum-containing NASICON-type materials with the general formula  $\text{Li}_{1-x}\text{Zr}_2\text{P}_{3-x}\text{Mo}_x\text{O}_{12}$  ( $x = 0, 0.1, 0.5, 1.0$ ).

Analysis of the catalytic properties of the synthesized compounds in ethanol conversion reactions has shown that all of them exhibit catalytic activity for ethanol dehydration and dehydrogenation reactions. The major reaction products are C2 hydrocarbons, C4 hydrocarbons, acetaldehyde, diethyl ether, and hydrogen. On the doped materials, we observed predominant formation of diethyl ether at low temperatures and C2 and C4 hydrocarbons at elevated temperatures. Doping with molybdenum reduces the reaction onset temperature on average by 60°C. In addition, the present results demonstrate that molybdenum-containing centers play a key role in the formation of acetaldehyde and hydrogen, because molybdenum can change its oxidation state and, accordingly, partic-

ipate in redox reactions. Increasing the molybdenum concentration leads to a decrease in the yield of the major reaction products, which seems to be related to the smaller specific surface area of the Mo-rich samples.

### ACKNOWLEDGMENTS

This work was supported by the Russian Foundation for Basic Research, grant no. 13-08-00660.

### REFERENCES

- Clark, J.H., Buldarin, V., Deswarte, F.I.E., Hardy, J.J.E., Kerton, F.M., Hunt, A.J., Luque, R., Macquarrie, D.J., Milkowski, K., Rodriguez, A., Samuel, O., Tavener, S.J., White, R.J., and Wilson, A.J., Green chemistry and the biorefinery: a partnership for a sustainable future, *Green Chem.*, 2006, vol. 8, pp. 853–860.
- Leach, B.E., *Applied Industrial Catalysis*, New York: Academic, 1983, vol. 2. Translated under the title *Kataliz v promyshlennosti*, Moscow: Mir, 1986, vol. 2, pp. 149–160.
- Hong, H.Y.-P., Crystal structures and crystal chemistry in the system  $\text{Na}_{1+x}\text{Zr}_2\text{Si}_x\text{P}_{3-x}\text{O}_{12}$ , *Mater. Res. Bull.*, 1976, vol. 11, no. 2, pp. 173–182.
- Agaskar, P., Grasselli, R., Buttrey, D., and White, B., Structural and catalytic aspects of some NASICON-based mixed metal phosphates, *Stud. Surf. Sci. Catal.*, 1997, vol. 110, pp. 219–225.
- Hong, H.Y.-P., Kafalas, J.A., and Bayard, M.L., High  $\text{Na}^+$ -ion conductivity in  $\text{Na}_5\text{YSi}_4\text{O}_{12}$ , *Mater. Res. Bull.*, 1978, vol. 3, no. 8, pp. 757–761.
- Kohler, H. and Schulz, H., NASICON solid electrolytes: Part I. The  $\text{Na}^+$ -diffusion path and its relation to the structure, *Mater. Res. Bull.*, 1985, vol. 20, no. 12, pp. 1461–1471.
- Yaroslavtsev, A.B. and Stenina, I.A., Complex phosphates with the NASICON structure ( $\text{A}_x\text{B}_2(\text{PO}_4)_3$ ), *Russ. J. Inorg. Chem.*, 2006, vol. 51, suppl. 1, pp. 97–116.
- Pet'kov, V.I., Mixed phosphates of metal cations in the oxidation states I and IV, *Usp. Khim.*, 2012, vol. 81, no. 7, pp. 606–637.
- Aramendia, M.A., Borau, V., Marinas, J.M., and Romero, F.J., The selectivity of  $\text{NaZnPO}_4$  in the dehydrogenation of the alcohol, *Chem. Lett.*, 1994, pp. 1361–1364.
- Serghini, A., Brochu, R., Ziyad, M., and Vadrine, J., Behaviour of copper–zirconium nasicon-type phosphate,  $\text{Cu}^{\text{I}}\text{Zr}_2(\text{PO}_4)_3$ , in the decomposition of isopropyl alcohol, *J. Chem. Soc., Faraday Trans.*, 1991, vol. 87, no. 15, pp. 2487–2493.
- Orlova, A.I., Pet'kov, V.L., Gul'yanova, S.T., Ermilova, M.M., Ienealem, S.L., Samuilova, O.K., Chekhlova, T.K., and Gryaznov, V.M., The catalytic properties of new complex zirconium and iron orthophosphates, *Russ. J. Phys. Chem. A*, 1999, vol. 73, no. 11, pp. 1767–1769.
- Brik, Y., Kacimi, M., Bozon-Verduraz, F., and Ziyad, M., Characterization of active sites on  $\text{AgHf}_2(\text{PO}_4)_3$  in butan-2-ol conversion, *Microporous Mesoporous Mater.*, 2001, vol. 43, pp. 103–112.
- Il'in, A.B., Novikova, S.A., Sukhanov, M.V., Ermilova, M.M., Orekhova, N.V., and Yaroslavtsev, A.B., Catalytic activity of NASICON-type phosphates for ethanol dehydration and dehydrogenation, *Inorg. Mater.*, 2012, vol. 48, no. 4, pp. 397–401.
- Mikhaleiko, I.I., Povarova, E.I., and Pylina, A.I., Copper-, cobalt-, and nickel-containing zirconium phosphate catalysts: synthesis, characterization, and surface properties, *Nauchn. Vedom. Belarus. Gos. Univ. Ser.: Mat. Fiz.*, 2012, no. 11 (130), pp. 169–174.
- Povarova, E.I., Pylina, A.I., and Mikhaleiko, I.I., Catalytic dehydrogenation of propanol-2 on Na-Zr phosphates containing Cu, Co, and Ni, *Russ. J. Phys. Chem. A*, 2012, vol. 86, no. 6, pp. 935–941.
- Pylina, A.I. and Mikhaleiko, I.I., Influence of compensator ions in the anionic part of  $\text{Na}_3\text{ZrM}(\text{PO}_4)_3$  phosphate with  $\text{M} = \text{Zn, Co, Cu}$  on the acidity and catalytic activity in reactions of butanol-2, *Russ. J. Phys. Chem. A*, 2013, vol. 87, no. 3, pp. 372–375.
- Pylina, A.I. and Mikhaleiko, I.I., Catalytic activity of thermally treated  $\text{Li}_3\text{Fe}_2(\text{PO}_4)_3$  in the conversion of butan-1-ol, *Mendeleev Commun.*, 2012, vol. 22, pp. 150–151.
- Pet'kov, V.I., Sukhanov, M.V., and Kurazhkovskaya, V.S., Feasibility of using crystalline NZP matrices for molybdenum immobilization, *Radiokhimiya*, 2003, vol. 45, no. 6, pp. 560–565.
- Pechini, M.P., US Patent 3 330 697, 1967.
- Kakihana, M. and Yoshimura, M., Synthesis and characterization of complex multicomponent oxides prepared by polymer complex method, *Bull. Chem. Soc. Jpn.*, 1999, vol. 72, pp. 1427–1443.
- Yaroslavtsev, A.B., *Khimiya tverdogo tela* (Solid State Chemistry), Moscow: Nauchnyi Mir, 2009.
- Sukhanov, M.V., Shchelokov, I.A., Ermilova, M.M., Orekhova, N.V., Pet'kov, V.I., and Tereshchenko, G.F., Catalytic properties of sodium zirconium molybdate phosphates in methanol transformations, *Russ. J. Appl. Chem.*, 2008, vol. 81, no. 1, pp. 17–22.

Translated by O. Tsarev